

**Dielectric Domain Distribution on Au Nanoparticles
Revealed by Localized Surface Plasmon Resonance**

Journal:	<i>Journal of Materials Chemistry C</i>
Manuscript ID	TC-ART-06-2018-002944.R1
Article Type:	Paper
Date Submitted by the Author:	20-Jul-2018
Complete List of Authors:	Luo, Yi; University of Connecticut, Chemistry Zhou, Yadong; University of Central Florida, Chemistry Zou, Shengli; University of Central Florida, Chemistry Zhao, Jing; University of Connecticut, Chemistry



Journal Name

ARTICLE

Dielectric Domain Distribution on Au Nanoparticles Revealed by Localized Surface Plasmon Resonance

Received 00th January 20xx,
Accepted 00th January 20xx

Yi Luo,^a Yadong Zhou,^b Shengli Zou,^b and Jing Zhao^{*a,c}

DOI: 10.1039/x0xx00000x

www.rsc.org/

Localized surface plasmon resonance (LSPR) of metal nanoparticles has been proven to be sensitive to their dielectric environment and molecular binding, but less is known about the capability of LSPR towards differentiating homogeneous versus segregated molecular distribution on the nanoparticle surface. Using silica on Au nanospheres to mimic the dielectric change caused by molecules on the nanosphere surface, we have discovered that the LSPR of Au nanospheres is sensitive to the distribution of dielectric domains. We grew discrete silica domains or a continuous shell on the Au nanosphere surface and observed that the discrete domains of silica induced very little shift in the LSPR while the uniform shell caused a drastic shift. Theoretical modeling further confirmed that even when the volume of the silica was kept the same, the discrete domains had much smaller impact on the LSPR of Au nanospheres than the continuous shell. Moreover, for an anisotropic Au nanorod, the simulation results show that the LSPR is more sensitive to the dielectric change at the ends ("hot spot") than the sides. The study suggests that the LSPR of metal nanoparticles can be conveniently used as an indirect method to reveal the dielectric distribution on the nanoparticles.

Introduction

Localized surface plasmon resonance, which is generated when light strikes a metal nanoparticle and induces collective oscillation of the conduction electrons of a noble metal nanoparticle, has been extensively studied over the past two decades.¹⁻⁵ LSPR of metal nanoparticles is dependent on various factors including composition, size, morphology, higher-order assembled structure, and local dielectric environment.⁶⁻¹⁶ Especially, the dielectric sensitivity of LSPR enables them to detect the binding of molecules on the surface of the metal nanoparticle, which causes spectral shift in both the extinction and scattering spectra.^{17,18} This feature of LSPR allows for the development of a great number of biosensors that detect molecular binding events.¹⁹⁻²²

Previous studies of the LSPR response of metal nanoparticles have demonstrated quantitatively how the amount of molecules or thickness of the dielectric layer on the nanoparticle would alter its LSPR both theoretically and experimentally.²³⁻³⁰ However, another factor that can impact LSPR but did not get too much attention is the location and distribution of the molecular/dielectric layer on the nanoparticle. In the work by Chen et al, it was discovered that Pd domains on Au nanorods would cause a redshift in the

LSPR while a continuous Pd shell would cause a blue shift due to the transition of the real part of the dielectric environment from positive to negative.³¹ However, how the distribution of a simple positive dielectric layer is not fully understood but still worth to be studied since dielectric domain segregation caused by inhomogeneous packing of molecules naturally occur on anisotropic metal nanoparticle surface due to the existence of crystal facets and curvatures.^{32,33} Even for a spherical metal nanoparticle capped with dual ligands, the molecules pack in striped or Janus patterns to reduce free energy.³⁴ One more specific case of non-uniform packing is the segregation of polymer brush caused by the change of solvent quality.³⁵⁻³⁷ Inspired by all these possible packing behaviours of molecules, we examine how the LSPR would respond to different distributions of the dielectric layer for better interpretation of LSPR shift in bio-sensing/detection. In addition, the packing of capping agents can heavily impact the site selective overgrowth of the coating material.^{32,33} The distribution of the ligands can also be manipulated to create anisotropy on isotropic nanospheres, enabling them to be directable building blocks for controlled assemblies.^{38,39} Different packing of surface ligands will also affect the cellular uptake behavior and therefore is of fundamental importance in biomedical applications.⁴⁰ Therefore, it is beneficial to investigate the capability of LSPR toward revealing the distribution of molecules on the nanoparticle surface. The positive results will allow LSPR to become an alternative to the current instrumentation extensive methods used to study molecular distribution at sub-100 nm regime, such as Electron Spin Resonance Spectroscopy, Nuclear Magnetic Resonance

^a Department of Chemistry, University of Connecticut, 55 North Eagleville Road, Storrs, CT 06269 (USA). E-mail: jing.zhao@uconn.edu

^b Department of Chemistry, University of Central Florida, 4104 Libra Drive, Orlando, Florida- 32816- 2366 (USA).

^c Institute of Material Science, University Of Connecticut, Storrs, CT 06269 (USA)
Electronic Supplementary Information (ESI) available: TEM and SEM images, and extinction spectra of Au-silica nanoparticles. See DOI: 10.1039/x0xx00000x

Spectroscopy, Atomic Force Microscopy and Scanning Tunnelling Microscopy.⁴¹⁻⁴⁵

Here we demonstrate how the segregation of dielectric material on Au nanoparticle surface would impact the LSPR using Au-silica structures as a case study. We also test the possibility of using the shift of LSPR to reveal the dielectric layer distribution on metal nanoparticles. Specifically, we change the reaction conditions in silica overgrowth to tune the Au-silica structure from core@shell to core-satellite to mimic uniform or segregated ligands. The surface coverage of silica domains in the core-satellite structure can also be controlled by changing the reaction time. Moreover, imaging of silica is also easily achievable with transmission electron microscopy (TEM), which provides direct evidence of the dielectric domain distribution on Au nanoparticles in addition to the LSPR measurement. The TEM imaging enables us to establish a direct correlation between the dielectric domain distribution and the LSPR response. Surprisingly, we discovered that with highly uniform Au nanospheres (Au NSs) as the core, the discrete silica domains caused almost no spectral shift in the UV-Vis spectra compared with that of the bare Au NSs. In stark contrast, a continuous silica shell of similar volume on the Au NSs induced a significant red-shift in the UV-Vis spectrum. Electrodynamics simulations of Au-silica structures agree with the experimental observations and show that when the dielectric domains are on the "hot spots" of the nanoparticles, a more drastic LSPR shift will be induced. The finding demonstrates that LSPR of Au nanoparticles is sensitive to the ligand distribution on the surface and can potentially be used as a convenient indirect method to study ligand binding and segregation on nanoparticles.

Experimental section

Chemicals and materials

Gold (III) chloride trihydrate ($\geq 99.9\%$ trace metals basis), sodium borohydride, L-ascorbic acid, hydroxylamine hydrochloride, hexadecyltrimethylammonium bromide (CTAB), cetyltrimethylammonium chloride solution (CTAC) (25% in water), 2-propanol (ACS reagent, $\geq 99\%$), poly (acrylic acid) (PAA) (average Mw=1800), 3-Mercaptopropionic acid (MPA) ($\geq 99\%$), and tetraethyl orthosilicate (TEOS) ($\geq 99.0\%$) were purchased from Sigma Aldrich. Ammonium hydroxide (28.0-30.0%) was purchased from J. T. Baker. All chemicals were used as received.

Synthesis of CTAC capped Au NSs

Synthesis of 117 nm CTAC capped Au NSs was adopted from Xia's group with slight modification.⁴⁶ The detailed procedure can be found in Luo, et al.⁴⁷ In general, the synthesis was divided into 4 parts: 1. Cluster growth, 2. Growth of 14 nm Au NS, 3. Growth of 40nm Au NS and 4. Growth of 117 nm Au NS.

Synthesis of Au-silica heterostructure/Au@silica core@shell structure

We adopted and modified the method developed by Chen et.al to synthesize Au-silica heterogeneous and Au@silica core@shell structures.⁴⁸ More detailed procedure can be found in

Luo, et al.⁴⁷ Briefly, 3 mL of the as prepared Au NS solution (5×10^{-11} M) were concentrated to 0.5 mL by centrifugation. The concentrated Au NS solution was added to 2.5 mL of 2-propanol. 20 μ L of MPA (5 mM in ethanol) and 20 μ L of PAA (0.645 mM in water) were then added to the solution (the PAA was eliminated in the synthesis of core@shell structure). The mixture was allowed to stir for 30 minutes. 600 μ L of TEOS (8.9 mM in ethanol for 42 nm Au-silica heterostructures, 20.7 mM in ethanol for 117 nm heterostructures) and 90 μ L of ammonium hydroxide were added afterwards. The reaction was kept under room temperature for certain amount of time for desired thickness/size (50 min-3 hours).

Transmission Electron Microscopy (TEM) Imaging

Au and Au-SiO₂ nanoparticles were transferred to a carbon-coated TEM grid (Electron Microscopy Sciences) for TEM imaging. FEI Tecnai G2 Spirit BioTWIN was used to acquire the TEM images under the acceleration voltage of 80 kV.

Scanning Electron Microscopy (SEM) Imaging

To prepare the SEM sample, 10 μ L of the sample was drop casted to a glass slide and left in air to dry. The glass slide was then coated with gold with a sputter coater to induce conductivity. FEI Nova NanoSEM 450 was used to acquire the SEM images.

UV-Vis spectra measurement

A UV-vis spectrometer (Cary 60, Agilent Technologies) was used to measure the extinction spectra of the Au NS and Au-silica structures.

Simulation

We used the discrete dipole approximation (DDA) method in the theoretical calculations. The detailed description of the method can be found in the reference.⁴⁹ In the DDA method, the target particle is divided into an array of polarizable cubes and the optical properties of any shaped particles can be calculated. The length of the cube was taken as 0.5 nm in all the simulations. The dielectric constants of gold were taken from Palik's handbook.⁵⁰ The refractive index of silica was 1.50.

Results and discussion

Effect of uniform vs segregated distribution of silica on LSPR

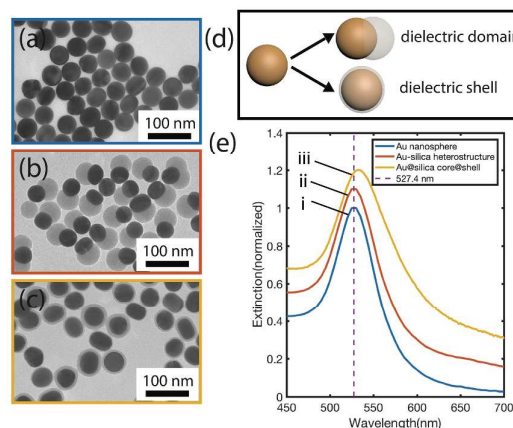


Figure 1: TEM images of a) 42 nm Au NS, b) 42 nm Au-silica heterostructure, c) 42 nm Au@silica core@shell, d) Schematic illustration of Au NS, Au-silica heterostructure and Au@silica core@shell structure, e) UV-Vis spectra of the corresponding structures.

Since the LSPR of a metal nanoparticle has been shown to be sensitive to its dielectric environment and ligand binding, we decided to test the capability of LSPR towards resolving the dielectric domain distribution around a nanoparticle. To do that, we synthesized two types of Au-silica structures: i.e. Au-silica heterostructure and Au@silica core@shell structure. Specifically, the Au@silica core@shell structure simulated a uniform layer of capping agents on Au NSs and the Au-silica heterostructure simulated the Janus or segregated distribution of capping agents (Figure 1d). The morphology of the bare Au NSs and Au-silica structures were characterized with TEM and the extinction spectra of the samples were measured in water (Figure 1). The TEM images in Figure 1a showed that the bare Au NSs have a diameter of 42 nm. The extinction spectrum of the Au NSs in water has a peak at 527.4 nm (Figure 1e(i)). The Au NSs were used as seeds and a silica domain of 52 nm in diameter was grown on the Au NSs, as illustrated in the TEM image in Figure 1b. Surprisingly, the extinction spectrum of Au-silica heterostructure showed almost no shift in the peak wavelength (527.6 nm, Figure 1e(ii)) compared to that of bare Au NPs. This is contradictory with the generally accepted theory that LSPR is affected by the local dielectric environment. In contrast, when the distribution of silica domain changed from a segregated single domain to a shell that has an average thickness of 4.8 nm, there is a red shift of the extinction peak to 534.3 nm (Figure 1e(iii)). We would like to emphasize that the volume of the silica domains are similar for the samples shown in Figure 1b and 1c. These observations demonstrate that a uniform dielectric layer close to the Au NP surface has a more significant impact on the LSPR than a segregated dielectric domain of similar or even larger volume.

Effect of multiple discrete silica domains on LSPR

In the cases when dual ligands are employed in nanoparticles simultaneously, the ligands don't necessarily segregate in a Janus pattern; instead, multiple domains may form. If the two ligands are distinctly different in molecular weight, the segregated pattern is analogous to having multiple discrete silica domains on the Au NS surface. In contrast, the random distribution of the two ligands is similar to a uniform silica shell covering the whole surface of the NS. To examine whether the LSPRs of metal nanoparticles can be used to distinguish the two cases, Au-silica structures of multiple discrete silica domains or a uniform shell were synthesized and compared. Specifically, 117 nm Au NSs (TEM image in Figure 2a) were employed as the seeds because it could support multiple discrete silica domain growth according to our previous study.⁴⁷ The silica domain size was controlled by the reaction time. The Au-silica heterogeneous structure that were synthesized in 1 hour of reaction had an average of 7 silica domains with a diameter of 50 nm based on the TEM image in Figure 2b. When the reaction proceeded for 1.5 hrs, silica size increased to a diameter of 63 nm (shown in the TEM image in Figure 2c). The synthesized Au-silica heterostructures with different domains sizes and Au@silica core@shell structures simulate different ligand patterns as illustrated in Figure 2e. UV-Vis spectra of the samples were acquired in water (Figure 2f) as a comparison. Similar to what was observed in the above case, the Au-silica heterostructure with 1 hr growth showed almost no shift in the LSPR peak compared with that of the bare Au NS (Figure 2f (i, ii), both peaked at 581.6 nm). The Au-silica heterostructure obtained from 1.5 hr of reaction had same number of silica domains as the 1 hr sample but bigger domain size. In this case we observed a small red-shift in the LSPR peak from 581.6 nm to 584.9 nm compared with the bare

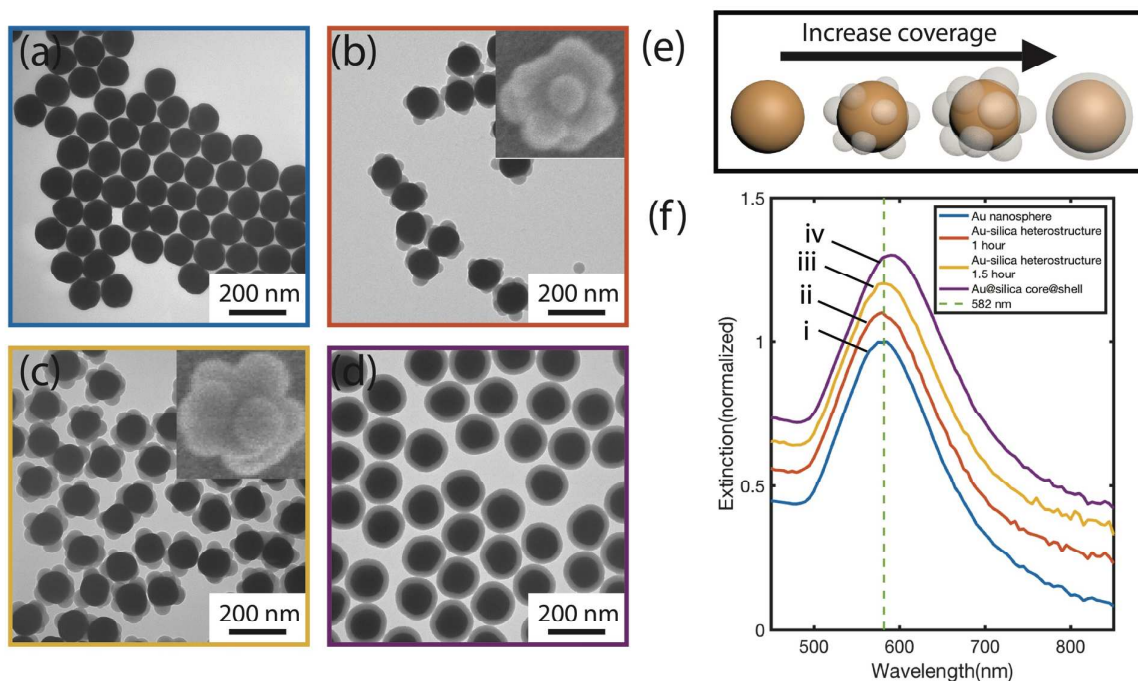


Figure 2: TEM images of a) 117 nm CTAC capped Au nanoparticle, 117 nm Au-silica heterostructure centrifuged after b) 1 hour of reaction, c) 1.5 hour of reaction, d) 117 nm Au@silica core@shell structure, e) Schematic illustration of corresponding structures, f) UV-Vis spectra of the corresponding structures.

Au NSs (Figure 2(iii)). As the silica grew in size, the height and contacting area with Au both increased. Since the plasmon decay length of Au nanoparticle is 5~15 nm,⁵¹ LSPR is the most sensitive to the dielectric environment change on the nanoparticle's surface. Therefore, we focus the following discussion on the surface coverage of silica in the different samples. There were 6 silica domains visible in the SEM image (Figure S1) on the Au NSs on average. We assumed there were two more domains hidden below the Au NS, making the total of 8 domains. The assumption is based on the Au core size and the silica domain diameter. We estimated that the contacting area of the 1 hr sample was 17665 nm² while the contacting area of the 1.5 hr sample was 28985 nm². As the surface area of a 117 nm Au in diameter can be easily calculated to be 42983 nm², the coverage of the 1 hr sample is calculated as 41% while the 1.5 hr sample is 67.4%. For the 40-60% surface coverage, the LSPR shift is observable but quite small. In contrast, Au@silica core@shell structure with a thin silica shell of 22 nm thickness (Figure 2d) showed a pronounced LSPR shift from 581.6 nm to 591.9 nm with 100% uniform coverage (Figure 2f(iv)). From our observations, we conclude that coating the Au NSs with discrete domains induced a small shift in the LSPR of Au NSs in comparison with a uniform coating on the entire surface. Although the experiments were performed on Au-silica system, the same conclusion will hold for other metal nanospheres with ligands or biomolecules.

Simulations of the LSPR of Au NS coated with silica domains

The phenomenon we observed where coating Au NSs with silica domains induced very small LSPR shift was contradictory with many previous studies. It has been demonstrated LSPR of Au nanoparticles is sensitive to molecular binding. To understand this unusual LSPR behaviour of the Au NSs, theoretical modeling was performed to simulate the experimental results and to provide information about the LSPR shift mechanism. Using the discrete dipole approximation (DDA) method,⁴⁹ we calculated the extinction spectra of Au spheres under different coating conditions in water. The details of the method can be found in the experimental section. To match the experimental results, the diameter of the Au sphere was set to 42 nm. In Figure 3a, we showed the extinction spectrum of an Au NS with a diameter of 42 nm in water. The extinction peak is at 531.5 nm, in good agreement with the experimental results in Figure 1e. In another simulation, we modeled the case where a silica domain with a 52 nm diameter was coated onto the Au sphere with a center to center distance of 42 nm, as illustrated in Figure 3a. To account for the random orientation of the Au-silica nanoparticles in solution, in the simulations, we randomly placed a silica particle near the Au sphere and carried out five simulations. The averaged extinction spectrum of the five simulations is presented in Figure 3a (ii). The resonance wavelength is only changed very slightly from 531.5 nm to 533.4 nm compared to that of the bare Au sphere. In stark contrast, when the Au NS is coated with a layer of silica with the same volume as that of a 52 nm diameter silica "sphere" (the "sphere" is incomplete in this case because the overlap

between the silica and Au as illustrated in Figure 3a), the resonance wavelength red shifted more pronouncedly from 531.5 to 541.2 nm. Notice that in the simulated results, when a silica domain was added to the side of the Au sphere, it induced a small red shift in the LSPR. But in the experimental results in Figure 1e, we did not observe any LSPR shift caused by the silica domain. This discrepancy mainly comes from the variations in the size of the Au NS and the silica domains. The measured extinction spectrum was essentially an averaged spectrum over a large number of Au-silica structures of slightly different morphologies. The small LSPR shift caused by silica domain was averaged out in the experimental measurement. Nevertheless, the simulated results agree with the experimental observations that a uniform silica coating caused much bigger LSPR shift than a silica domain of similar volume. To further investigate the effect of dielectric domain distribution on LSPR, we compared the extinction spectra of Au NSs when they are coated with two silica spheres with different amount of overlap between silica and Au NS. In the simulations, the sizes of the Au sphere and silica sphere remain the same as in the previous simulations. For the structure in Figure 3b that corresponds to the spectrum ii in Figure 3b, the center to center distance between the silica domain and the Au NS was set at 42 nm. Again, the two silica domains were randomly arranged near the Au NS. Five simulations were carried out to obtain the averaged results. In comparison to that of the bare Au sphere, the resonance wavelength of the Au NS coated with two silica domains is only shifted from 531.5 to 534.9 nm. However, when a layer of silica with the same volume of the two incomplete silica spheres was coated on the Au NS surface, the resonance wavelength is further red shifted to 543.3 nm (Figure 3b (iv)). Quite interestingly, when we randomly placed two silica spheres with a center to center distance between the Au and silica spheres of 21 nm (the scheme corresponding to

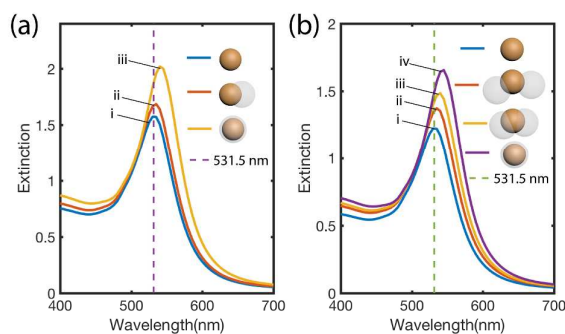


Figure 3: a) simulated extinction spectra of bare Au sphere (i, blue spectrum), Au with one silica domain (ii, red spectrum) and Au with a silica shell (iii, yellow spectrum). b) simulated extinction spectra of bare Au sphere (i, blue spectrum), Au and two silica domain with a small overlap (ii, red spectrum), Au and two silica domain with a large overlap (iii, yellow spectrum) and Au with a silica shell (iv, purple spectrum).

spectrum iii in Figure 3b), the volume of the coated silica spheres is less than the case when the center to center distance was at 42 nm, due to the larger overlap between the Au NS and silica domains. However, the resonance wavelength showed a bigger redshift to 538.2 nm. The simulated results demonstrate that the total volume of silica is not the critical factor in determining the LSPR shift. Instead, how much silica is in direct contact or in close proximity to the surface has a more significant role in inducing LSPR shift.

From both the experimental and theoretical results, the LSPR of Au NSs is more sensitive to the immediate dielectric domains to the surface of the Au. The volume or thickness of the dielectric layer has less impact on the LSPR compared to the surface coverage. It is still surprising that there was almost no shift in the LSPR when the silica domains were coated on Au nanoparticles in some cases. We attribute it to the following reason. The Au nanoparticles we used are spherical in shape. Previous works have demonstrated the spheres have the least LSPR sensitivity compared to particles with high aspect ratios or sharp tips and edges.⁵² We expect that if the nanoparticles are more rod-like, the LSPR will be more sensitive to segregated dielectric domains. To demonstrate this effect experimentally, we synthesized Au nanoparticles using citrate acid instead of CTAC as the ligand. The nanoparticles have an average diameter of 120 nm, similar to that of the nanoparticles in Figure 2. The citrate capped nanoparticles are quasi-spherical or rod-like in shape and have a faceted surface instead of being spherical (Figure S2). When one or two small silica domains were grown onto the nanoparticles, a LSPR shift from 590.0 nm to 592.8 nm was observed. In comparison, the CTAC capped Au NSs showed almost no shift in the LSPR when small silica domains were coated onto them. The LSPR was then further shifted to 594.0 nm as we increased the number of silica domains. This control experiment showed that the irregular shaped Au nanoparticles are more sensitive to the dielectric domains.

Simulations of the LSPR of Au nanorod coated by silica domains

The Au NSs we used in the experiments have an aspect ratio of 1. To determine the LSPR sensitivity to the ligands of nanostructures with higher aspect ratio, we also calculated the resonance wavelength of an Au rod when it was coated with silica at different positions, i.e. sides vs. ends. Such structures have been first reported by Wang's and Murphy's groups.^{32,33} The rod length was selected as 30 nm and the diameter was 10 nm. Two silica spheres were coated at the two ends of the rod with a diameter of 15 nm which represent a 2.5 nm thick silica at the two ends of the rod. The structure is illustrated in Figure 4a scheme (ii). In another calculation, a spheroidal silica particle with diameters of 18.5, 18.5, and 19 nm was coated at the center of the rod (scheme (iii) in Figure 4a). The volume of the coated silica was the same in two simulations. The calculated extinction spectra of the longitudinal mode are shown in Figure 4a and the complete spectra are available in Figure S3. The resonance wavelength is shifted from 708 nm for the bare rod to 716 nm when the silica was coated on the sides of the rod and further to 729 nm when the silica domains

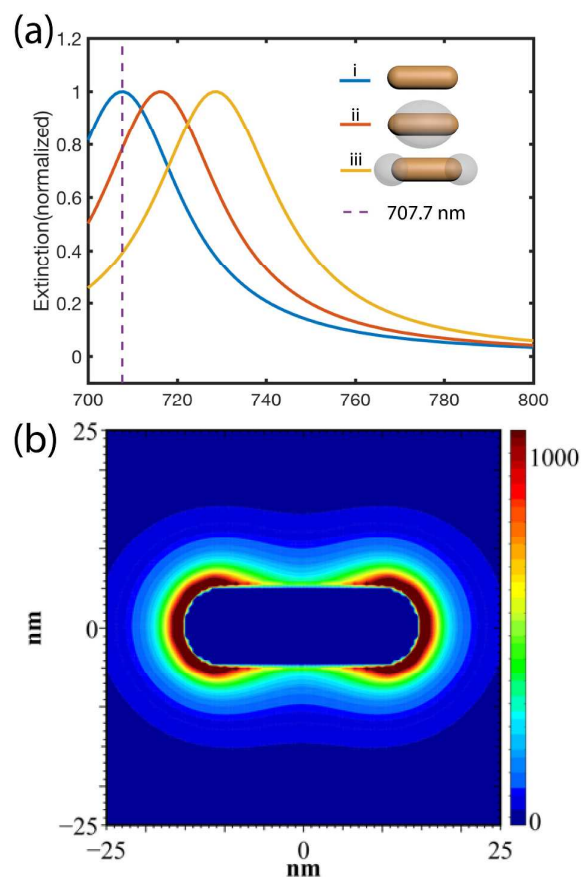


Figure 4: (a) simulated extinction spectra of a Au nanorod (i), Au rod with silica coated on the side (ii) and Au rod with silica coated at the ends (iii). (b) electric field contour plot for the bare rod at the resonance wavelength of 708 nm.

were coated at the two ends. We also calculated the electric field distribution of the bare rod at the resonance wavelength of 708 nm which is shown in Figure 4b. The electric field contour plot indicates that the enhanced local electric fields are much higher at the two ends. The high electric field makes the impact of silica coating at the ends of the rods on LSPR more significant than the case when silica was coated to the sides with lower electric field. Therefore, LSPR is more sensitive to ligand binding to the "hot spots" compared to elsewhere. This finding is in agreement with the experimental results reported by Wang's group.³² Szekreñyes et.al discovered that after small molecules (cysteamine) replaced the bulky polyethylene glycol (PEG) at the tips of a PEGylated gold nanorod, the LSPR showed a pronounced blue shift from 640 nm to 628 nm.⁴⁴ Zhu et.al's work showed similar results as well. The coating of silica at the ends of Au nanobipyramids caused greater spectral red-shift compared with silica coating on the side.⁵³ Whitney et.al also showed that the sharp feature (an "apron" of Ag at the bottom) of the a Ag hemispheroid created a stronger near field and induced greater LSPR sensitivity toward the local dielectric change.²⁴ All the

experimental and theoretical studies demonstrate that LSPR can be used as an indirect tool to study ligand distribution and molecular binding on metal nanoparticles.

Conclusions

In this work, experimental and theoretical studies were performed on Au-silica nanostructures where the silica domain distribution was controlled. The system was used to mimic segregated/uniform ligand distribution on metal nanoparticles. We found that the LSPR of the Au nanoparticles depends on the distribution of the silica domain instead of volume of the silica domains. Specifically, segregated domains at one side of the Au nanoparticle induced much less (or almost no) LSPR shift compared to the uniformly distributed domain of the same or even smaller volume. Dielectric domains at the “hot spots” induce much greater LSPR shift than elsewhere. The conclusions from this work can be broadly applied to many plasmonically-active metal nanoparticles to reveal the ligand and dielectric layer distribution on these nanoparticles.

Conflicts of interest

There are no conflicts to declare.

Acknowledgements

We acknowledge the financial supported by NSF CAREER Grant (CHE 1554800). The electron microscopy imaging work was performed at the Biosciences Electron Microscopy Facility of the University of Connecticut.

References

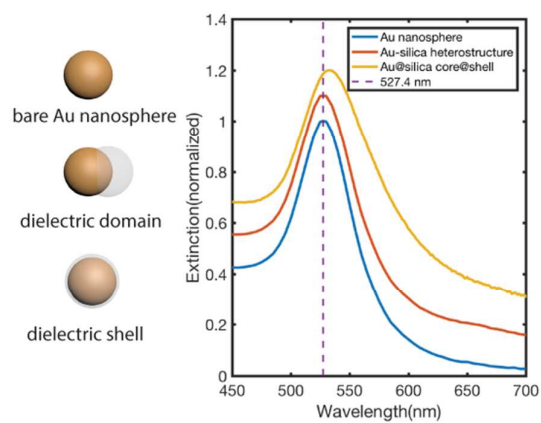
- 1 M. Faraday, *Philosophical Transactions of the Royal Society of London*, 1857, **147**, 145-181.
- 2 U. Kreibig and M. Vollmer, *Optical properties of metal clusters*, Springer Science & Business Media, 2013.
- 3 K. L. Kelly, E. Coronado, L. L. Zhao and G. C. Schatz, *Journal*, 2003.
- 4 S. Link and M. A. El-Sayed, *Annu. Rev. Phys. Chem.*, 2003, **54**, 331-366.
- 5 S. Eustis and M. A. El-Sayed, *Chem. Soc. Rev.*, 2006, **35**, 209-217.
- 6 U. Kreibig and L. Genzel, *Sur. Sci.*, 1985, **156**, 678-700.
- 7 J. Mock, M. Barbic, D. Smith, D. Schultz and S. Schultz, *J. Chem. Phys.*, 2002, **116**, 6755-6759.
- 8 C. L. Haynes and R. P. Van Duyne, *Journal*, 2001.
- 9 E. Hutter and J. H. Fendler, *Adv. Mater.*, 2004, **16**, 1685-1706.
- 10 W. A. Murray and W. L. Barnes, *Adv. Mater.*, 2007, **19**, 3771-3782.
- 11 V. Myroshnychenko, J. Rodríguez-Fernández, I. Pastoriza-Santos, A. M. Funston, C. Novo, P. Mulvaney, L. M. Liz-Marzan and F. J. G. de Abajo, *Chem. Soc. Rev.*, 2008, **37**, 1792-1805.
- 12 C. Novo, A. M. Funston, I. Pastoriza-Santos, L. M. Liz-Marzan and P. Mulvaney, *J. Phys. Chem. C*, 2008, **112**, 3-7.
- 13 Y. Luo, L. Dube, Y. Zhou, S. Zou and J. Zhao, *Prog. Nat. Sci. Mat. Int.*, 2016, **26**, 449-454.
- 14 S. Thota, S. Chen, Y. Zhou, Y. Zhang, S. Zou and J. Zhao, *Nanoscale*, 2015, **7**, 14652-14658.
- 15 J. A. Jenkins, Y. Zhou, S. Thota, X. Tian, X. Zhao, S. Zou and J. Zhao, *J. Phys. Chem. C*, 2014, **118**, 26276-26283.
- 16 X. Tian, Y. Zhou, S. Thota, S. Zou and J. Zhao, *J. Phys. Chem. C*, 2014, **118**, 13801-13808.
- 17 J. Piella, N. G. Bastús and V. Puntès, *Chem. Mater.*, 2016, **28**, 1066-1075.
- 18 K. M. Mayer and J. H. Hafner, *Chem. Rev.*, 2011, **111**, 3828-3857.
- 19 K. A. Willets and R. P. Van Duyne, *Annu. Rev. Phys. Chem.*, 2007, **58**, 267-297.
- 20 S. Szunerits and R. Boukherroub, *Chem. Commun.*, 2012, **48**, 8999-9010.
- 21 B. Sepúlveda, P. C. Angelomé, L. M. Lechuga and L. M. Liz-Marzán, *nano today*, 2009, **4**, 244-251.
- 22 M. Shen, A. A. Joshi, R. Vannam, C. K. Dixit, R. G. Hamilton, C. V. Kumar, J. F. Rusling and M. W. Peczu, *ChemBioChem*, 2018.
- 23 J. J. Mock, D. R. Smith and S. Schultz, *Nano Lett.*, 2003, **3**, 485-491.
- 24 A. V. Whitney, J. W. Elam, S. Zou, A. V. Zinovev, P. C. Stair, G. C. Schatz and R. P. Van Duyne, *J. Phys. Chem. B*, 2005, **109**, 20522-20528.
- 25 T. Rindzevicius, Y. Alaverdyan, M. Käll, W. A. Murray and W. L. Barnes, *J. Phys. Chem. C*, 2007, **111**, 11806-11810.
- 26 M. Duval Malinsky, K. L. Kelly, G. C. Schatz and R. P. Van Duyne, *J. Phys. Chem. B*, 2001, **105**, 2343-2350.
- 27 E. Galopin, J. Niedziółka-Jönsson, A. Akjouj, Y. Pennec, B. Djafari-Rouhani, A. Noual, R. Boukherroub and S. Szunerits, *J. Phys. Chem. C*, 2010, **114**, 11769-11775.
- 28 S. K. Ghosh, S. Nath, S. Kundu, K. Esumi and T. Pal, *J. Phys. Chem. B*, 2004, **108**, 13963-13971.
- 29 S. Link, M. Mohamed and M. El-Sayed, *J. Phys. Chem. B*, 1999, **103**, 3073-3077.
- 30 L. J. Sherry, R. Jin, C. A. Mirkin, G. C. Schatz and R. P. Van Duyne, *Nano Lett.*, 2006, **6**, 2060-2065.
- 31 H. Chen, F. Wang, K. Li, K. C. Woo, J. Wang, Q. Li, L.-D. Sun, X. Zhang, H.-Q. Lin and C.-H. Yan, *ACS nano*, 2012, **6**, 7162-7171.
- 32 F. Wang, S. Cheng, Z. Bao and J. Wang, *Angew. Chem. Int. Ed.*, 2013, **52**, 10344-10348.
- 33 J. G. Hinman, J. R. Eller, W. Lin, J. Li, J. Li and C. J. Murphy, *J. Am. Chem. Soc.*, 2017, **139**, 9851-9854.
- 34 P. K. Ghorai and S. C. Glotzer, *J. Phys. Chem. C*, 2010, **114**, 19182-19187.
- 35 R. B. Grubbs, *Polym. Rev.*, 2007, **47**, 197-215.
- 36 Y. Wang, J. He, C. Liu, W. H. Chong and H. Chen, *Angew. Chem. Int. Ed*, 2015, **54**, 2022-2051.
- 37 S. Zhang, G. Leem, L.-o. Srisombat and T. R. Lee, *J. Am. Chem. Soc.*, 2008, **130**, 113-120.
- 38 T. Chen, M. Yang, X. Wang, L. H. Tan and H. Chen, *J. Am. Chem. Soc.*, 2008, **130**, 11858-11859.
- 39 C. P. Shaw, D. G. Fernig and R. Lévy, *J. Mater. Chem*, 2011, **21**, 12181-12187.
- 40 V. Schubertová, F. J. Martínez-Veracoechea and R. Vácha, *Soft Matt.*, 2015, **11**, 2726-2730.
- 41 C. Gentilini and L. Pasquato, *J. Mater. Chem*, 2010, **20**, 1403-1412.
- 42 X. Liu, M. Yu, H. Kim, M. Mameli and F. Stellacci, *Nature Commun.*, 2012, **3**, 1182.

Journal Name

ARTICLE

- 43 C. Gentilini, P. Franchi, E. Mileo, S. Polizzi, M. Lucarini and L. Pasquato, *Angew. Chem. Int. Ed.*, 2009, **48**, 3060-3064.
- 44 D. P. Szekrenyes, S. Pothorszky, D. Zámbo, Z. Osváth and A. Deák, *The Journal of Physical Chemistry C*, 2018.
- 45 A. M. Jackson, Y. Hu, P. J. Silva and F. Stellacci, *J. Am. Chem. Soc.*, 2006, **128**, 11135-11149.
- 46 Y. Zheng, X. Zhong, Z. Li and Y. Xia, *Particle & Particle Systems Characterization*, 2014, **31**, 266-273.
- 47 Y. Luo, S. Geng; L. Dube; J. Zhao, *J. Phys. Chem. C*, 2018, in press.
- 48 T. Chen, G. Chen, S. Xing, T. Wu and H. Chen, *Chem. Mater.*, 2010, **22**, 3826-3828.
- 49 B. T. Draine and P. J. Flatau, *JOSA A*, 1994, **11**, 1491-1499.
- 50 A. D. Rakić, A. B. Djurišić, J. M. Elazar and M. L. Majewski, *Appl. Opt.*, 1998, **37**, 5271-5283.
- 51 A. J. Haes, S. Zou, G. C. Schatz and R. P. Van Duyne, *J. Phys. Chem. B*, 2004, **108**, 109-116.
- 52 A. U. Khan, S. Zhao and G. Liu, *The Journal of Physical Chemistry C*, 2016, **120**, 19353-19364.
- 53 X. Zhu, H. Jia, X. M. Zhu, S. Cheng, X. Zhuo, F. Qin, Z. Yang and J. Wang, *Adv. Funct. Mater.*, 2017, **27**, 1700016.

Table of Contents



The LSPR of Au nanosphere shows almost no shift in the extinction spectrum with attachment of a silica domain but considerable shift with a uniform layer of silica, indicating LSPR can be used to differentiate the segregated/uniform dielectric distribution.